RESEARCH ARTICLE OPEN ACCESS

Glycerol Bioconversion into Bioethanol: A Comparative Analysis of Microbial Growth and Structural Adaptation



ISSN: 1874-0707

Herliati Rahman^{1,*}, Flora Elvistia Firdaus¹, Yeti Widyawati¹, Luthfia Hastiani Muharram², Nida Nabilah¹ and Alfiona Ismail¹

¹Department of Chemical Engineering, Faculty of Industrial Technology, Jayabaya University, Jalan Raya Bogor km 28,8 Jakarta Timur 16452, Indonesia

²Department of Biotechnology, Muhammadiyah University of Bandung, Jalan Soekarno - Hatta No. 752 Cipadung Kidul, Panyileukan, Bandung, Indonesia

Abstract:

Introduction: Glycerol, the main byproduct of biodiesel production, poses environmental challenges if not effectively utilized. Converting glycerol into bioethanol provides a sustainable route to support renewable energy development. This study explores the potential of microbial isolates with high lipase activity for efficient glycerol fermentation.

Methods: The tested strains included three bacteria (Serratia sp., Pseudomonas sp., Escherichia coli), one yeast (Saccharomyces sp.), and two fungi (Aspergillus sp., Trichoderma sp.). Morphological adaptations were evaluated using Scanning Electron Microscopy (SEM), and ethanol production was validated through Fourier-Transform Infrared (FT-IR) spectroscopy by identifying characteristic absorption peaks. Quantitative analysis of ethanol yield and glycerol conversion was conducted using High-Performance Liquid Chromatography (HPLC).

Results: SEM analysis confirmed structural adaptation of *Serratia sp.* and *Saccharomyces sp.* under fermentation stress. FT-IR analysis verified the presence of ethanol with an absorption peak at 3251.52 cm⁻¹. HPLC results showed that *Serratia sp.* produced the highest ethanol yield of 17.83% (5.35 g/L) with a glycerol conversion of 40.33%, followed by *Trichoderma sp.* with a yield of 17.37% (5.21 g/L) and a conversion of 39.56%. Although *E. coli* exhibited the highest glycerol conversion (80.54%), its ethanol yield was low (1.88%), indicating diversion toward other metabolic pathways.

Discussion: These results highlight the superior adaptability and metabolic efficiency of *Serratia sp.* in channeling glycerol toward ethanol production. Structural stability under osmotic and ethanol stress supports its role as a robust bioethanol producer, while differences among species underscore the importance of strain-specific optimization.

Conclusion: Serratia sp. demonstrates strong potential for glycerol-to-bioethanol conversion, providing a promising candidate for sustainable biofuel production and biodiesel waste valorization.

Keywords: Bioethanol, Microbial adaptation, Renewable energy, SEM, FT-IR, Sustainability.

© 2025 The Author(s). Published by Bentham Open.

This is an open access article distributed under the terms of the Creative Commons Attribution 4.0 International Public License (CC-BY 4.0), a copy of which is available at: https://creativecommons.org/licenses/by/4.0/legalcode. This license permits unrestricted use, distribution, and reproduction in any medium, provided the original author and source are credited.

*Address correspondence to this author at the Department of Chemical Engineering, Faculty of Industrial Technology, Jayabaya University, Jalan Raya Bogor km 28,8 Jakarta Timur 16452, Indonesia; E-mail: herliatimulyono@gmail.com

Cite as: Rahman H, Firdaus F, Widyawati Y, Muharram L, Nabilah N, Ismail A. Glycerol Bioconversion into Bioethanol: A Comparative Analysis of Microbial Growth and Structural Adaptation. Open Biotechnol J, 2025; 19: e18740707396790. http://dx.doi.org/10.2174/0118740707396790251015065015



Received: March 02, 2025 Revised: July 13, 2025 Accepted: August 26, 2025 Published: October 17, 2025



Send Orders for Reprints to reprints@benthamscience.net

1. INTRODUCTION

Bioethanol production from biodiesel waste glycerol is a significant alternative to providing renewable energy [1, 2]. In this context, glycerol is the main byproduct of biodiesel production and accounts for about 10% of the total output. Therefore, the surplus glycerol generated has become an economic and environmental challenge with the global increase in biodiesel production [3, 4]. A sustainable solution is provided by turning glycerol into bioethanol because the compound is frequently impure and has no economic value [5, 6]. This procedure reduces the environmental effect of producing biodiesel while converting waste streams into valuable fuel [7, 8]. Bioethanol is produced through biomass fermentation starting from the first generation and has been known as environmentally friendly alternative energy to conventional fossil fuels. This renewable fuel offers several advantages, including significantly reducing Greenhouse Gas (GHG) emissions [9, 10]. According to the United States (U.S.) Department of Energy report, bioethanol reduces CO2 emissions by up to 34% compared to fossil gasoline, depending on the production methods and biomass sources used [1]. This renewable fuel contributes to climate change mitigation by reducing dependence on fossils [3]. The photosynthesis process in bioethanolproducing plants absorbs CO₂ from the atmosphere to offset emissions generated when bioethanol is used [11].

Based on the explanation, bioethanol is important in the global transition to sustainable energy [12, 13] and can be directly used in vehicles without significant modification. This is an advantage in a faster transition to renewable energy use [14]. The conversion of glycerol into bioethanol creates value from waste and closes the biodiesel production cycle to improve the overall economic feasibility [7, 15]. Previous research showed that glycerol conversion efficiency could reach more than 90% under optimized fermentation conditions [16]. Reducing waste and enhancing the economic value of raw materials through bioethanol production can improve the profitability of the biodiesel industry. This situation enables producers to invest in sustainable and efficient technologies [17, 18].

The yeast cerevisiae has long been recognized as a microorganism capable of converting glycerol into ethanol through fermentation [19]. However, the effectiveness and efficiency of the process are influenced by fermentation conditions and the ability of the microorganism to adapt to the glycerol substrate. Several studies have examined the role of Saccharomyces cerevisiae and the bacterium Escherichia coli as fermentation agents in bioethanol production [20, 21]. However, exploration of the potential of other bacteria, such as Serratia and Pseudomonas aeruginosa, as well as fungi including Trichoderma and Aspergillus niger, remains limited.

This research observed the morphological adaptation of microorganisms during glycerol metabolism, using color changes and the turbidity level of the fermentation medium as initial indicators of metabolic activity [22].

Scanning Electron Microscopy (SEM) served as the principal method for high-resolution micrograph analysis, facilitating the examination of microorganism surface structures, morphological alterations, and microbial interactions within the fermentation environment [23]. The SEM method effectively identifies structural changes indicative of microbial adaptation to the glycerol substrate. A combination of visual, microscopy, spectroscopic, and chromatographic methods was used to assess the effectiveness of glycerol fermentation and the morphological differences among the involved microbial strains. Fourier-Transform Infrared (FT-IR) spectroscopy was applied to identify the ethanol spectrum produced, confirming the successful bioconversion of glycerol into Additionally, High-Performance Chromatography (HPLC) was used to quantitatively identify glycerol and ethanol after fermentation [24]. The results could be an alternative reference for improving bioethanol production from biodiesel byproducts.

2. METHODOLOGY

This research was designed to evaluate microbial growth and morphology during glycerol fermentation into bioethanol and to identify the ethanol produced through spectroscopic and chromatographic analysis. The stages included the preparation of materials and reagents, followed by glycerol fermentation using three bacterial (*Pseudomonas* sp., *Serratia* sp., and *Escherichia coli*) and fungal strains (*Saccharomyces* sp., *Aspergillus* sp., and *Trichoderma* sp.) [4]. Subsequently, analyses were conducted using SEM, FT-IR, and HPLC to observe morphological changes in the microorganisms, determine the ethanol spectrum produced, and conduct quantitative analysis.

2.1. Microbial Strains and Culture Preparation

A total of six microbial strains that have high lipase activity (5.01-6.26 mU/g) were selected for the potential in glycerol bioconversion, namely Serratia sp., Saccharomyces cerevisiae, Pseudomonas sp., Escherichia coli, Aspergillus sp., and Trichoderma sp. Re-culturing microbes obtained from earlier research rejuvenated bacterial and fungal isolates [4]. Bacterial colonies were purified by transferring them with an inoculation loop on Nutrient Agar plates and incubated for 24 hours. This process obtained a pure culture sample of lipolytic bacteria. The yeast isolate rejuvenation method was also adapted from previous research. Purification was performed by transferring yeast colonies with an inoculation loop onto plates containing PDA (Potato Dextrose Agar) medium, followed by incubation for 3-4 days. This method led to a pure culture sample of lipolytic yeast [25].

Microorganisms developed from previous research [4] are stored and rejuvenated in the genomic laboratory of the National Research and Innovation Agency of Indonesia. For bacterial inoculum preparation, Luria Bertani (LB) medium was used. LB medium consists of peptone (10 g/L), yeast extract (5 g/L), and sodium chloride (10 g/L), providing the necessary nutrients to support rapid and robust bacterial growth. Each bacterial isolate was pre-cultured by

inoculating 10 mL into a 200 mL Erlenmeyer flask containing 100 mL sterile LB medium. Cultures were incubated at 30°C and agitated at 150 rpm for 7 days. After incubation, bacterial cultures were centrifuged at 6000 rpm for 10 minutes at room temperature to obtain the cell pellets used for fermentation [26].

This research used the Potato Dextrose Broth (PDB) medium for the growth of yeast and fungi [27]. PDB was prepared by dissolving it in distilled water, then homogenizing and sterilizing it using an autoclave at 121°C for 15 minutes to ensure the medium was free from contamination. Subsequently, the pure isolate was aseptically inoculated into a sterile PDB medium, and the incubation was conducted for 10 days at 30°C or room temperature. After the incubation, the culture was separated using Whatman No. 1 sterile filter paper (pore size 11 μm) to collect the culture broth or enzymes produced by the yeast. All microbial strains were maintained under the same respective media conditions throughout the study to ensure comparability of growth and fermentation performance.

2.2. Fermentation Setup and Conditions

The glycerol fermentation process starts by mixing 200 mL of 30% (w/w) glycerol solution with 100 mL of microbial culture prepared in a medium rich in nutrients such as nitrogen, phosphorus, and other essential minerals. This mixture was inoculated with selected microorganisms, including three bacterial strains (Pseudomonas sp., Serratia sp., and Escherichia coli) and three fungal strains (Saccharomyces sp., Aspergillus sp., and Trichoderma sp.), recognized for the ability to convert glycerol into ethanol [4]. Fermentation occurs at a temperature of 40°C and a pH of 4-5 for 3 days based on the optimal growth and activity conditions for the microorganisms. Visual observations were conducted daily for 3 days to evaluate color changes and turbidity during fermentation. After 72 hours, samples were taken and separated into supernatant and solid. The solid was analyzed using SEM, while the supernatant was examined qualitatively and quantitatively using FT-IR and HPLC, respectively. This method evaluated the potential of microbes in converting glycerol to ethanol, which helped in the bioconversion process.

2.3. High-performance Liquid Chromatography (HPLC) Analysis

The type of HPLC used was Waters Alliance, Shimadzu Shimpack GIST C18 (4.6 mm x 250 mm, 5 µm), UV/VIS detector operated at a wavelength of 210 nm [28]. Meanwhile, a mixture of 95% water and 5% acetonitrile was used as the mobile phase. The elution process was carried out isocratically, with a fixed mobile phase composition during the analysis, allowing consistent and efficient separation of analytes [29]. The injection volume used was 20 µL, sufficient to provide a good signal response to the detector without causing overload on the column. The mobile phase flow rate was set at 0.5 mL/min, and the column temperature was constant at 80°C. This temperature condition was selected to maintain the stability of analyte retention and ensure the detection of ethanol without being affected by temperature fluctuations [30]. The sample was filtered with a 0.1 µm filter paper to avoid contamination or solid particles damaging the HPLC column. Ethanol was identified by comparing the retention time of sample peaks to the required standard, with the retention time observed at approximately 11.19 minutes.

Ethanol quantification was achieved by constructing a calibration curve using standard solutions of known concentrations. The area under the peak corresponding to ethanol in the chromatogram was measured and compared to the calibration curve to determine the concentration. Meanwhile, the reproducibility of the HPLC results was verified by performing duplicate analyses for each sample. Fermentation yields and glycerol conversion were determined using Eqs. (1 and 2), respectively.

$$\% Yield = \frac{[E]}{[G]_0} x100$$
 (1)

% Conversion =
$$\frac{[G]_0 - [G]_f}{[G]_0} \times 100$$
 (2)

Where $[G]_0$ is the substrate's starting concentration of glucose 30% (mg/mL), $[G]_f$ is the substrate's final concentration of glucose, and [E] is the concentration of ethanol in the fermentation broth (mg/mL) [31].

2.4. Scanning Electron Microscopy (SEM) Analysis

The sample preparation for SEM analysis starts with centrifuging the fermentation product at 8,000 rpm and 4°C for 10 minutes to separate the pellet from the supernatant. The pellet is collected and sterilized by immersing it in a 96% glutaraldehyde solution for 24 hours to prevent microbial spread on the equipment and to ensure safety. After disinfection, the microbial pellet was separated from the glutaraldehyde solution. The samples were dried using a critical point dryer and coated with gold-palladium before observation under a JEOL JSM-6510 SEM at magnifications up to $10,000 \times [32]$.

2.5. Fourier Transform Infrared Spectroscopy (FT-IR) Analysis

Bioethanol production was confirmed by FT-IR spectroscopy (PerkinElmer Frontier), with spectral resolution set at 4 cm $^{-1}$ and scanning range 4000–500 cm $^{-1}$. The FTIR sample was clarified by centrifugation at 8000 rpm, followed by filtration through a 0.22 µm sterile membrane filter. Compared to standard ethanol spectra, ethanol presence was determined by the absorption peak at $\sim\!1050$ cm $^{-1}$ (C-O stretching) and $\sim\!3300$ cm $^{-1}$ (O-H stretching). Additionally, a liquid nitrogen-cooled MCT-A detector was also available with a Universal Attenuated Total Reflectance (UATR) [33].

2.6. Statistical Analysis

All experimental data were collected in duplicate and expressed as mean ± Standard Deviation (SD). One-way Analysis of Variance (ANOVA) was conducted to evaluate significant differences among microbial treatments regarding ethanol yield and glycerol conversion. When significant differences were detected, Tukey's post-hoc test was applied to identify pairwise differences between

groups, using a significance level of p < 0.05. All statistical analyses were performed using IBM SPSS Statistics software (IBM Corp., Armonk, NY, USA).

2.7. Research Diagram

Figure 1 shows the overall process of bioethanol synthesis and characterization from glycerol. This diagram provides an overview of microbial fermentation, ethanol production, and analytical characterization using SEM and FT-IR

3. RESULTS AND DISCUSSION

3.1. HPLC Calibration for Glycerol and Ethanol Ouantification

The accuracy and precision of glycerol and ethanol quantification were validated using HPLC. Table ${\bf 1}$

presents the linear range, regression equations, coefficients of determination (R²), and Limits of Detection (LOD) for glycerol and ethanol. The high R^2 values (\geq 0.9978) show strong linear correlations between concentration and peak area, ensuring reliable quantification. The calibration for glycerol followed the equation y = 2.8332E + 06x + 1.9842E + 06, with an R^2 value of 0.9978, indicating a strong linear correlation and high precision in detecting the concentrations within the tested range. Similarly, the ethanol calibration produced the equation y = 30,981.5x + 14,025.5, with an R^2 value of 0.9983, reflecting an excellent fit for quantifying the concentrations [34]. These equations were used to calculate the residual glycerol and ethanol concentrations in the fermentation broth, enabling precise determination of conversion rates and yields for evaluating microbial efficiency.

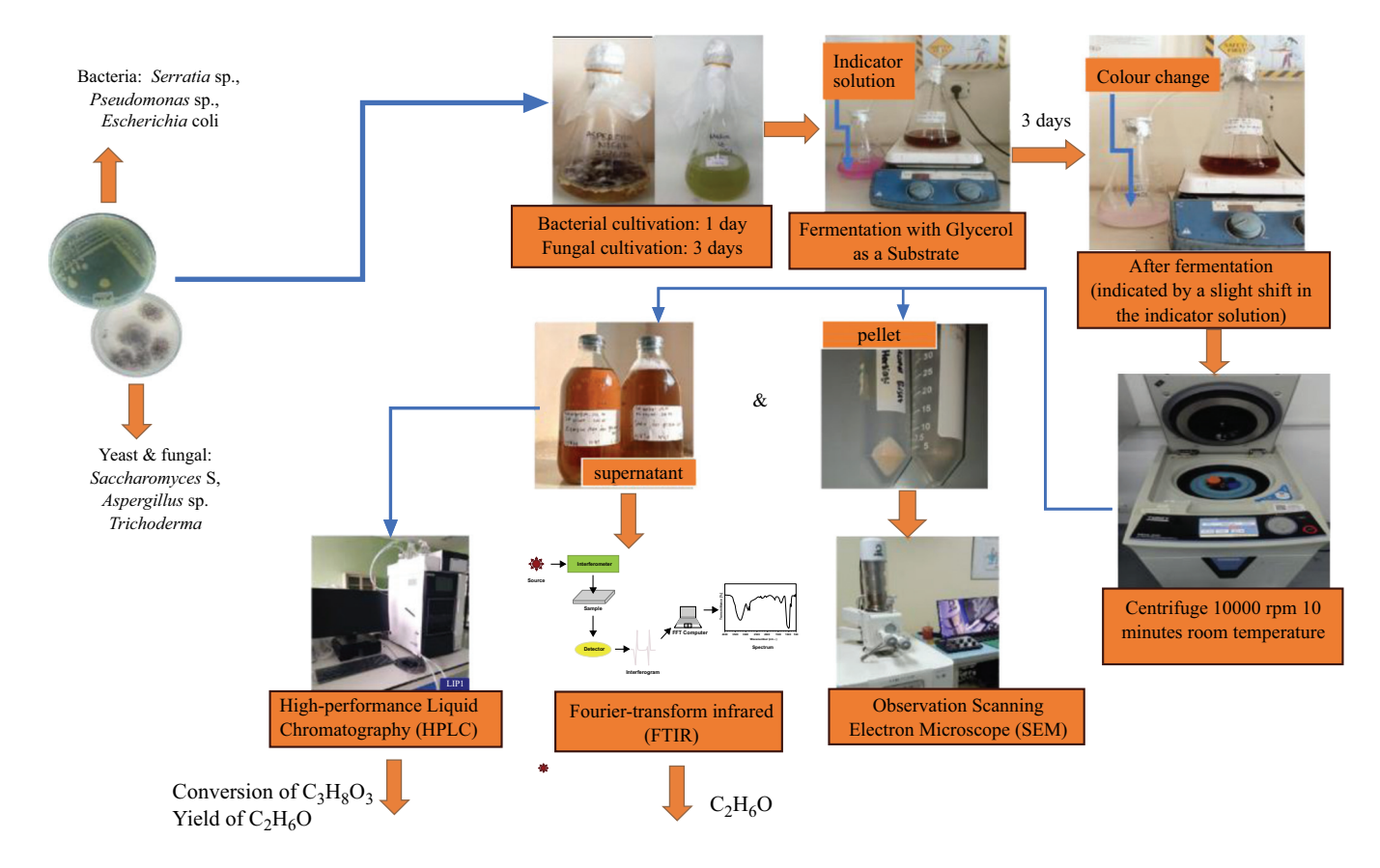


Fig. (1). Diagram of bioethanol synthesis and characterization from glycerol.

Table 1. Linear range, regression equation, coefficient of determination (R^2), and limit of detection (LOD) for glycerol and ethanol quantification *via* HPLC.

Component	Concentration (g/L)	Regression Equation	\mathbb{R}^2	LOD (mg/L)
Glycerol	1-20 g/L	y = 2.8332E + 06x + 1.9842E + 06	0.9978	98.4
Ethanol	1-20 g/L	y = 30,981.5x + 14,025.5	0.9983	98.4

Table 2. Quantitative analysis of glycerol conversion and ethanol yield by various microorganisms using HPLC
after 3 days of fermentation (T = 40° C, pH = 4, initial substrate concentration = 30% , (w/v).

Microbial Strain	Ethanol Yield (g/L)	Glycerol Conversion (%)
Serratia sp.	5.35 ± 0.12 ^a	40.33
Trichoderma sp.	5.21 ± 0.15 ^a	39.87
Saccharomyces cerevisiae	$4.89 \pm 0.11^{\text{b}}$	38.45
Pseudomonas sp.	3.76 ± 0.09 °	29.42
Aspergillus sp.	3.45 ± 0.08 °	27.88
Escherichia coli	2.89 ± 0.07 ^d	23.75

Note: Superscript letters (a , b , c) indicate significant differences among the ethanol yield means. Values sharing the same letter are not significantly different, while values with different letters are significantly different at p < 0.05.

3.2. Ethanol Production and Microbial Performance

The ethanol production results varied across microbial strains, with Serratia sp. and Trichoderma sp. reporting the highest yield of 17.83% (5.35 g/L) and 17.37% (5.21 g/L), as well as 40.33% and 39.56% conversion rate of glycerol, respectively. In contrast, $Escherichia\ coli$ showed the lowest ethanol production due to suboptimal metabolic pathways for glycerol fermentation. According to Table 2, quantitative analysis using HPLC after 3 days of fermentation confirmed the results, with $Serratia\$ sp. reported as the most efficient candidate. Statistical analysis was conducted using one-way ANOVA, followed by Tukey's posthoc test, to validate the reproducibility and significant differences among ethanol yields of tested strains (p < 0.05).

Based on the quantitative analysis using HPLC, Serratia sp. demonstrated the best performance in synthesizing bioethanol from glycerol compared to other microbes, including Trichoderma sp., Pseudomonas aeruginosa, Saccharomyces cerevisiae, Aspergillus sp., and Escherichia coli. Serratia sp. achieved a glycerol conversion rate of 40.33%, producing the highest ethanol concentration of 5.35 g/L and a yield of 17.83%. This high yield shows the metabolic efficiency of Serratia sp. in channeling glycerol as a substrate for ethanol production. The results are consistent with [35], reporting Serratia sp. as an effective bacterium for ethanol synthesis under stress conditions induced by substrate toxicity.

Trichoderma sp. reported an ethanol yield, concentration, and glycerol conversion rate of 17.37%, 5.21 g/L, and 39.56%, respectively. These results were consistent with other studies [36], which reported the potential of the species for bioethanol production but with slower substrate utilization compared to bacterial strains. Conversely, Escherichia coli showed the highest glycerol conversion rate of 80.54% and achieved an ethanol yield of 1.88%. In this context, a significant portion of glycerol was diverted to non-ethanol metabolites, as reported by Adnan et al. [37]. The research reported a similar trend, with Escherichia coli converting 80% of glycerol and yielding only 3.4% to reinforce the limited ethanol production efficiency despite high substrate utilization [38].

Other microbes, such as *Pseudomonas aeruginosa*, *Saccharomyces cerevisiae*, and *Aspergillus* sp., showed lower ethanol yields at 17.13%, 5.70%, and 2.31%,

respectively. These observations were consistent with a previous study [39], which reported lower ethanol productivity of *Aspergillus* species due to a preference for secondary metabolites over ethanol. The structural integrity and metabolic activity of *Serratia* sp. during fermentation were validated through SEM. The results showed that *Serratia* sp. maintained a stable and healthy cell structure under conditions of high osmotic pressure and potential ethanol toxicity. This condition was consistent with Wang *et al.*'s research [14], who emphasized the robustness of *Serratia* sp. in challenging fermentation environments.

Figure 2 shows the HPLC chromatogram of the *Serratia* bacterial performance. The retention time of 11.19 minutes corresponds to a key metabolite produced during fermentation, potentially indicating ethanol synthesis. Meanwhile, the additional peaks observed at retention times of 9.924 and 12.980 minutes suggest the presence of intermediate compounds or byproducts. The chromatogram analysis confirms the production of bioethanol and provides insight into the metabolic pathways. The retention time at 11.19 minutes is consistent with reported values for ethanol, showing the successful conversion of glycerol into bioethanol under the conditions used.

3.3. Microbial Morphology, Structural Adaptations, and Optimization Potential

SEM was used to observe the structure of microorganisms after fermentation, enabling an evaluation of cell morphological changes due to the glycerol metabolism process. JEOL JSM 7610F SEM uses Field Emission Gun (FEG) technology, which enables high resolution and good contrast for detailed analysis of microbial samples. This high-resolution microscope provides a visualization of microbial surface structures, allowing a comprehensive observation of morphological changes and microbial interactions in the fermentation environment. SEM is essential for evaluating microbial adaptation to glycerol substrates and reporting structural variations during fermentation. Figure 3 shows the morphological structure of Serratia at three different magnifications. At 2,500× (Fig. 3a), the colony exhibits an overall dense and tightly connected structure with visible pores and intercellular spaces that support glycerol fermentation activity. This adaptation allows for more efficient metabolite exchange and colony stability during fermentation.

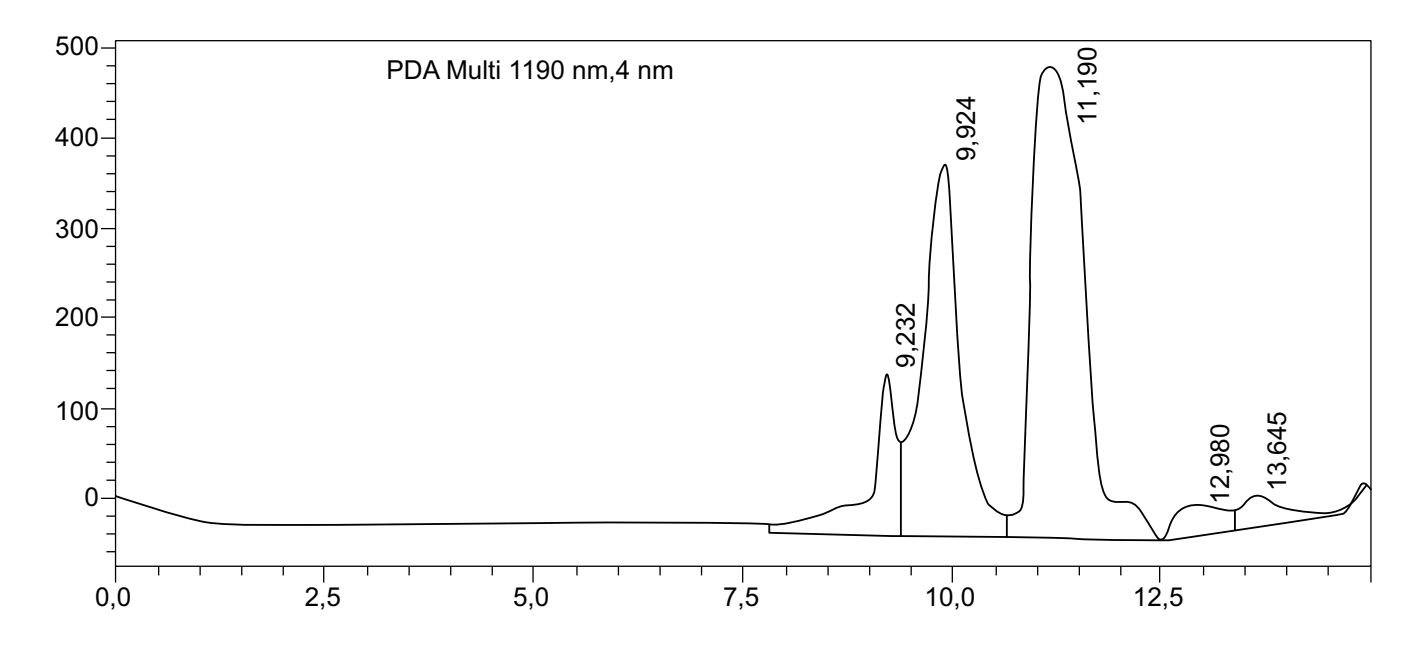


Fig. (2). HPLC chromatogram showing the performance of *Serratia* bacteria in glycerol fermentation. A retention time of 11.19 minutes indicates ethanol production.

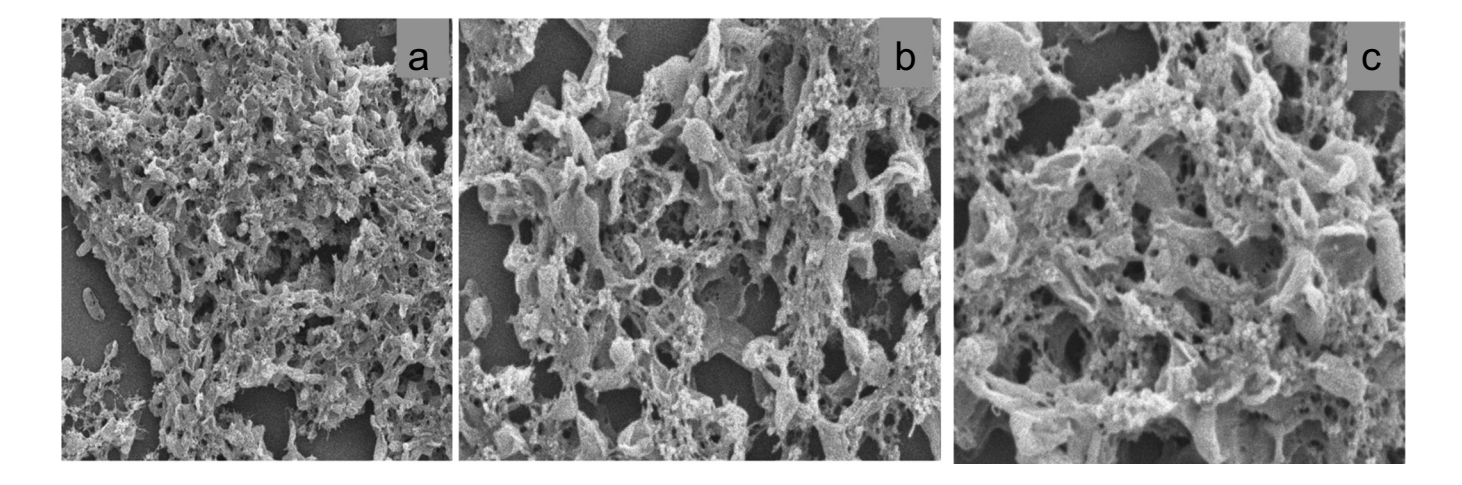


Fig. (3). SEM test results of Serratia at different magnifications: (a) 2,500×, (b) 5,000×, and (c) 10,000×.

The pores and gaps between the colonies show environmental adaptations allowing Serratia cells to interact at 5000x magnification (Fig. 3b), and the structure of the intercellular network is visible. The bacterial colonies appear to adhere and bond to each other, forming denser aggregates in the fermentation environment used. Therefore, the details of the surface structure of the cell network are more visible at 10,000x magnification (Fig. 3c). Pores are visible on the colony walls, and magnification reveals a smooth surface layer with small spaces between bacterial colonies.

Microbes conduct cell remodeling to adapt and tolerate higher ethanol, as reported by Wang et al. [14].

Meanwhile, microbial cells act as fine fibers around the surface due to the shrinkage phase, which is common in the fermentation process caused by osmotic pressure and nutrient fluctuations [40]. Osmotic pressure occurs in the early fermentation phase, namely, the substrate with a high sugar content, while the final phase has a high ethanol content. The membrane blebbing phase is characterized by irregular protrusions to produce Bacterial Extracellular Vesicles (BEVs) and plays an important role during fermentation [41].

To enhance the ethanol productivity of *Serratia* sp., further optimization strategies can be considered, including strain improvement *via* mutagenesis or adaptive

laboratory evolution, as well as metabolic engineering to redirect more carbon flux toward ethanol synthesis. Additionally, fermentation parameters such as aeration, agitation, and co-substrate supplementation (e.g., nitrogen sources or cofactors) can be fine-tuned to increase yield. Previous studies have also shown that immobilization techniques or co-cultivation with yeast could improve overall fermentation efficiency [37]. While Serratia sp. shows superior adaptability, it is also important to explore the potential of other isolates, such as Trichoderma sp. or Pseudomonas sp., by optimizing growth media, pH ranges, or implementing fed-batch strategies to support longer fermentation cycles. Such efforts would broaden the microbial candidates available for bioethanol production from glycerol and reduce reliance on a single strain.

3.4. FT-IR Spectroscopy Analysis of Ethanol Production

Ethanol spectrum analysis was performed using a PerkinElmer Frontier FT-IR with UATR. This instrument is capable of directly analyzing samples without complex preparation. It is suitable for non-destructive processes, such as confirming the presence of ethanol compounds through specific absorption peaks in the infrared spectrum. Figure 4 presents the FT-IR spectrum of

ethanol produced by Serratia during glycerol fermentation at 40°C, pH 4-5, over 72 hours. The broad and intense absorption band at 3272.13 cm $^{-1}$ corresponds to O-H stretching, a hallmark of alcohol functional groups. The band at 2889.7 cm $^{-1}$ is attributed to C-H stretching from alkyl chains. The absorption near 1458.31 cm $^{-1}$, although typically associated with -CH $_2$ scissoring or bending vibrations, is often present in both glycerol and ethanol spectra. The band at 924.55 cm $^{-1}$, commonly reported as an indicator of C-OH bending in secondary alcohols, overlaps with glycerol's own strong absorptions, necessitating careful spectral interpretation.

To distinguish ethanol from residual glycerol, comparative reference spectra and prior literature were consulted. Previous studies [42] report that ethanol typically exhibits strong absorptions in the 3200–3300 $\rm cm^{-1}$ (O-H) and 2800–2900 $\rm cm^{-1}$ (C-H) regions, with moderate bands between 1000–1100 $\rm cm^{-1}$ for C-O stretching. Although some overlap exists with glycerol, the presence of all three defining features (O-H, C-H, and C-O) in conjunction with fermentation-specific shifts suggests the formation of ethanol. It is also noted that the ethanol assignments were further validated through parallel HPLC quantification.

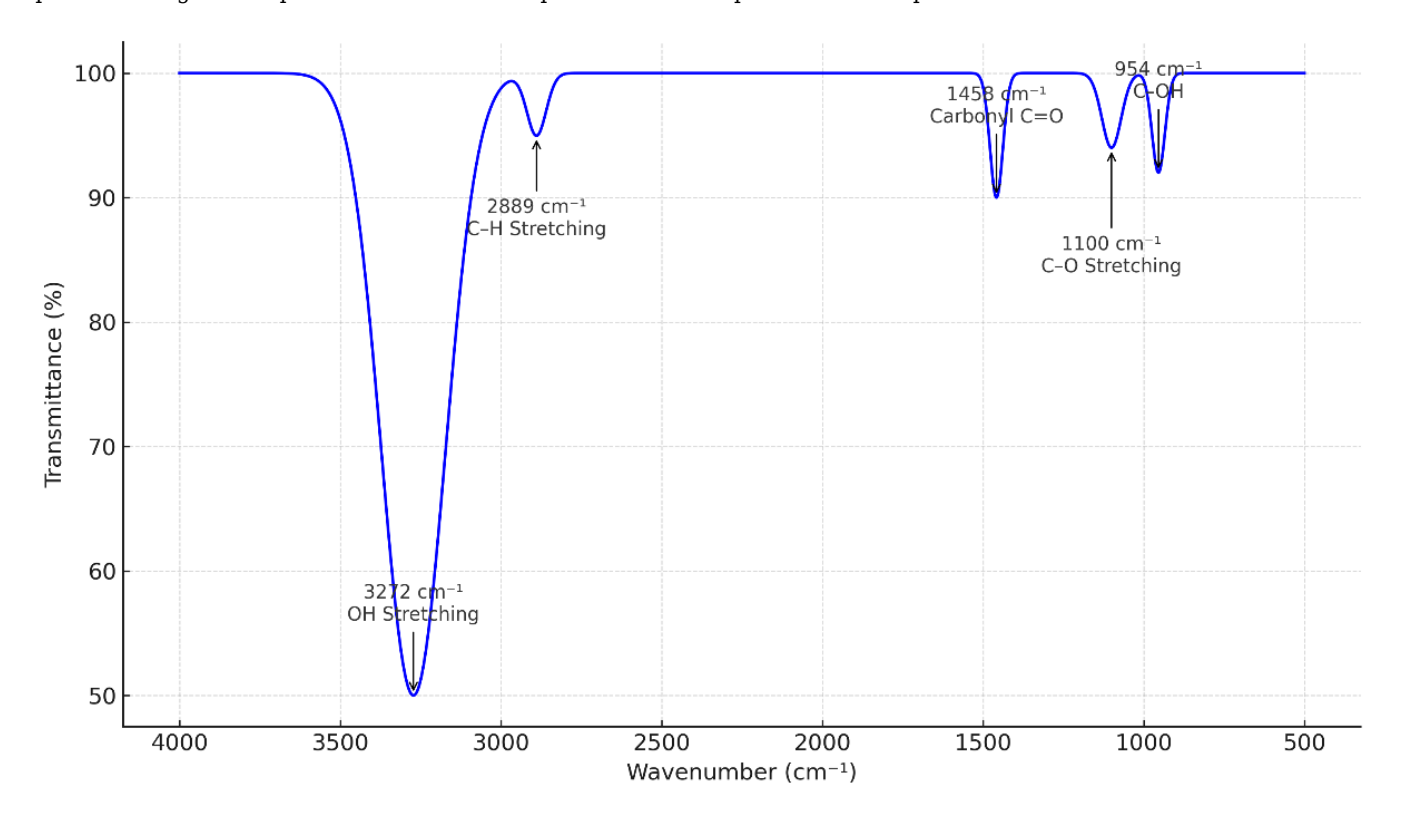


Fig. (4). FTIR spectrum of ethanol produced by Serratia during glycerol fermentation (T = $40 \,^{\circ}$ C; pH = 4-5; 72 hours). The characteristic absorption bands correspond to OH stretching (3272.13 cm⁻¹), C-H stretching (2889.7 cm⁻¹), carbonyl C=O (1458.31 cm⁻¹), C-OH bending (954.55 cm⁻¹), and C-O stretching.

CONCLUSION

In conclusion, Saccharomyces cerevisiae and Serratia sp. showed superior fermentation performance, indicated by color changes and increased medium turbidity, reflecting elevated metabolic activity and effective adaptation to glycerol. Scanning Electron Microscopy (SEM) validated these findings by revealing structural integrity and morphological adaptations in Serratia sp. and S. cerevisiae, including pore formation and cell aggregation, which suggest tolerance to ethanol accumulation and osmotic stress. Additionally, morphological observations in Trichoderma sp. also indicated adaptation capabilities, although SEM images were less pronounced than in the top-performing strains. FT-IR analysis confirmed the presence of ethanol at an absorption peak of 3251.52 cm⁻¹, showing successful bioconversion of glycerol into bioethanol. Quantitative analysis using HPLC showed that Serratia reported the best performance compared to Trichoderma. Pseudomonas aeruainosa. Aspergillus, and Escherichia coli. Serratia survived in the fermentation environment of glycerol into bioethanol with a yield of 17.83%. These results provided a strong foundation for further research to optimize the use of Serratia.

Despite these promising results, this study has several limitations. The fermentation was conducted under a fixed set of laboratory conditions (30-40°C, pH 4-5, 3-day duration), which may not fully reflect industrial-scale applications or performance variability under different environmental conditions. Moreover, ethanol quantification was limited to endpoint analysis; dynamic monitoring of fermentation kinetics was not conducted. While SEM and FT-IR provided valuable structural and spectral insights, they do not quantify cellular viability or stress response at the molecular level. Future research should incorporate omics-based approaches, continuous fermentation systems, and scale-up validation to optimize bioethanol production from glycerol using *Serratia* sp. and other microbial candidates.

AUTHORS' CONTRIBUTIONS

The authors confirm contribution to the paper as follows: H.R.: Conceptualization, methodology, writing, review editing, supervision, and funding; F.E.F.: Methodology, validation, data analysis, and curation; Y.W.: Methodology, validation, and data analysis; A.I. and N.N.: Preparation, experiment, and investigation. All authors have read and agreed to the published version of the manuscript.

LIST OF ABBREVIATIONS

BEVs = Bacterial Extracellular Vesicles

FT-IR = Fourier-Transform Infrared Spectroscopy

GHG = Greenhouse Gas

HPLC = High-Performance Liquid Chromatography

LB = Luria Bertani (medium)

LOD = Limit of Detection

PDB = Potato Dextrose Broth

PDA = Potato Dextrose Agar

 R^2 = Coefficient of Determination

SD = Standard Deviation

SEM = Scanning Electron Microscopy

UATR = Universal Attenuated Total Reflectance

ETHICS APPROVAL AND CONSENT TO PARTICIPATE

This study involved microbial cultures only and did not include any human participants or animal subjects. Therefore, ethical approval was not required in accordance with institutional and national research regulations.

HUMAN AND ANIMAL RIGHTS

Not applicable.

CONSENT FOR PUBLICATION

Not applicable.

AVAILABILITY OF DATA AND MATERIALS

The data supporting the findings of this article are available at the following link: https://drive.google.com/drive/folders/1DMW05z6L1pfCnw5kmYG07bW_Uxzjkd7K?usp=sharing

FUNDING

This research was funded by the Research Technology-National Research and Innovation Agency (RISTEK-BRIN) under the Research Contract for the 2024 Fiscal Year, LLDIKTI Research Contract with Jayabaya University: 801/LL3/AL.04/2024, Researcher Research Contract: SP DIPA-105/E5/PG.02.00.PL/2024.

CONFLICT OF INTEREST

The authors declare no conflict of interest, financial or otherwise.

ACKNOWLEDGEMENTS

The authors are grateful to Research Technology-National Research and Innovation Agency (RISTEK-BRIN) for funding the research under the Research Contract for the 2024 Fiscal Year, Number: LLDIKTI research contract with Jayabaya University: 801/LL3/AL.04/2024, Researcher research contract SP DIPA-105/E5/PG.02.00.PL/2024.

REFERENCES

- [1] Kassim MA, Meng TK, Kamaludin R, Hussain AH, Bukhari NA. Bioprocessing of sustainable renewable biomass for bioethanol production. Value-Chain of Biofuels. Amsterdam, Netherlands: Elsevier 2022; pp. 195-234. http://dx.doi.org/10.1016/B978-0-12-824388-6.00004-X
- [2] Pothu R, Mameda N, Boddula R, Mitta H, Perugopu V, Al-Qahtani N. Sustainable conversion of biodiesel-waste glycerol to acrolein over Pd-modified mesoporous catalysts. Mater Sci Energy Technol 2023; 6: 226-36.

- http://dx.doi.org/10.1016/j.mset.2022.12.012
- [3] Lari GM, Pastore G, Haus M, et al. Environmental and economical perspectives of a glycerol biorefinery. Energy Environ Sci 2018; 11(5): 1012-29.
 - http://dx.doi.org/10.1039/C7EE03116E
- [4] Zulaika A, Rahman H, Ningrum SS, Maulida AF. Exploring microbial lipases: Screening and identification for biocatalyst potential in bioethanol synthesis from glycerol-based biodiesel waste. Results Eng 2024; 23: 102427. http://dx.doi.org/10.1016/j.rineng.2024.102427
- [5] Rahman H, Nehemia A, Astuti HP. Investigating the potential of avocado seeds for bioethanol production: A study on boiled water delignification pretreatment. Inter J Renew Energy Devel 2023; 12(4): 648-54.
 - http://dx.doi.org/10.14710/ijred.2023.52532
- [6] Lopes AP, Souza PR, Bonafé EG, Visentainer JV, Martins AF, Canesin EA. Purified glycerol is produced from the frying oil transesterification by combining a pre-purification strategy performed with condensed tannin polymer derivative followed by ionic exchange. Fuel Process Technol 2019; 187: 73-83. http://dx.doi.org/10.1016/j.fuproc.2019.01.014
- [7] Ningaraju C, Yatish KV, Prakash R, Mithun SM, Balakrishna RG. Simultaneous refining of biodieselderived crude glycerol and synthesis of value-added powdered catalysts for biodiesel production: A green chemistry approach for sustainable biodiesel industries. J Clean Prod 2022; 363: 132448. http://dx.doi.org/10.1016/j.jclepro.2022.132448
- [8] Šalić A, Kučan KZ, Gojun M, Rogošić M, Zelić B. Biodiesel purification: Real-world examples, case studies, and current limitations. Sustainable Biodiesel. Amsterdam, Netherlands: Elsevier 2023; pp. 185-237. http://dx.doi.org/10.1016/B978-0-12-820361-3.00005-X
- [9] Jhang SR, Lin YC, Chen KS, Lin SL, Batterman S. Evaluation of fuel consumption, pollutant emissions and well-to-wheel GHGs assessment from a vehicle operation fueled with bioethanol, gasoline and hydrogen. Energy 2020; 209: 118436. http://dx.doi.org/10.1016/j.energy.2020.118436
- [10] Johansson R, Meyer S, Whistance J, Thompson W, Debnath D. Greenhouse gas emission reduction and cost from the United States biofuels mandate. Renew Sustain Energy Rev 2020; 119: 109513.
 - http://dx.doi.org/10.1016/j.rser.2019.109513
- [11] Chisti Y. Biodiesel from microalgae. Biotechnol Adv 2007; 25(3): 294-306.
 - http://dx.doi.org/10.1016/j.biotechadv.2007.02.001 PMID: 17350212
- [12] Haji Esmaeili SA, Szmerekovsky J, Sobhani A, Dybing A, Peterson TO. Sustainable biomass supply chain network design with biomass switching incentives for first-generation bioethanol producers. Energy Policy 2020; 138: 111222. http://dx.doi.org/10.1016/j.enpol.2019.111222
- [13] Zhao M, Wang Y, Zhou W, Zhou W, Gong Z. Co-valorization of crude glycerol and low-cost substrates via oleaginous yeasts to micro-biodiesel: Status and outlook. Renew Sustain Energy Rev 2023; 180: 113303. http://dx.doi.org/10.1016/j.rser.2023.113303
- [14] Wang C, Chang D, Zhang Q, Yu Z. Enhanced bioethanol production by evolved Escherichia coli LGE2-H in a microbial electrolysis cell system. Bioresour Bioprocess 2024; 11(1): 4. http://dx.doi.org/10.1186/s40643-023-00717-5 PMID: 38647898
- [15] Karimi K, Khoshnevisan B, Denayer JFM. Critical impacts of energy targeting on the sustainability of advanced biobutanol separation. Biof Res J 2024; 11(1): 1999-2012. http://dx.doi.org/10.18331/BRJ2024.11.1.2
- [16] de Ruijter JC, Frey AD. Analysis of antibody production in Saccharomyces cerevisiae: Effects of ER protein quality control disruption. Appl Microbiol Biotechnol 2015; 99(21): 9061-71. http://dx.doi.org/10.1007/s00253-015-6807-7 PMID: 26184977
- [17] Caffrey KR, Veal MW, Chinn MS. The farm to biorefinery continuum: A techno-economic and LCA analysis of ethanol

- production from sweet sorghum juice. Agric Syst 2014; 130: 55-66.
- http://dx.doi.org/10.1016/j.agsy.2014.05.016
- [18] Khan TMY. Direct transesterification for biodiesel production and testing the engine for performance and emissions run on biodiesel-diesel-nano blends. Nanomaterials 2021; 11(2): 417. http://dx.doi.org/10.3390/nano11020417 PMID: 33562116
- [19] Jetti KD, Gns RR, Garlapati D, Nammi SK. Improved ethanol productivity and ethanol tolerance through genome shuffling of Saccharomyces cerevisiae and Pichia stipitis. Int Microbiol 2019; 22(2): 247-54. http://dx.doi.org/10.1007/s10123-018-00044-2 PMID: 30810988
- [20] Cofré O, Ramírez M, Gómez JM, Cantero D. Optimization of culture media for ethanol production from glycerol by Escherichia coli. Biomass Bioenergy 2012; 37: 275-81. http://dx.doi.org/10.1016/j.biombioe.2011.12.002
- [21] Mueansichai T, Rangseesuriyachai T, Thongchul N, Assabumrungrat S. Lignocellulosic bioethanol production of napier grass using trichoderma reesei and saccharomyces cerevisiae co-culture fermentation. Inter J Renew Energy Devel 2022; 11(2): 423-33. http://dx.doi.org/10.14710/ijred.2022.43740
- [22] Choudhary OP, Kalita PC, Doley PJ, Kalita A. Scanning electron microscope: Advantages and disadvantages in imaging components. Life Sci Leafl 2018; 289-311.
- [23] Khan MSI, Oh SW, Kim YJ. Power of scanning electron microscopy and energy dispersive x-ray analysis in rapid microbial detection and identification at the single cell level. Sci Rep 2020; 10(1): 2368. http://dx.doi.org/10.1038/s41598-020-59448-8 PMID: 32047250
- [24] Jaramillo L, Pazutti LB, de-Aguiar PF, Ferreira-Leitão VS, Sérvulo EC. Determination of metabolites involved in natural succinic acid production from glucose, glycerol and crude glycerin by HPLC methodology. Rev Mex Ing Quim 2019; 19(2): 653-67. http://dx.doi.org/10.24275/rmig/Bio747
- [25] Zulaika A, Rachma Wijayanti D, Safari W F. A preliminary study of soil microbial abundance in succulent plant rhizospheres. Biota 2021; 14(1): 34-45. http://dx.doi.org/10.20414/jb.v14i1.340
- [26] Yamamoto K, Toya S, Sabidi S, Hoshiko Y, Maeda T. Diluted Luria-Bertani medium vs. sewage sludge as growth media: Comparison of community structure and diversity in the culturable bacteria. Appl Microbiol Biotechnol 2021; 105(9): 3787-98. http://dx.doi.org/10.1007/s00253-021-11248-4 PMID: 33856534
- [27] Rahman S, Jahan N, Sultana S, Adhikary SK, Yasmin S. Evaluation of the growth performance of trichoderma harzianum (Rifai.) on different culture media. 2013. Available from: https://www.researchgate.net/publication/326405457_Evaluation_ Of_The_Growth_Performance_Of_Trichoderma_harzianum_Rifai_O n_Different_Culture_Media
- [28] Puszkiel A, Plé A, Huillard O, et al. A simple HPLC-UV method for quantification of enzalutamide and its active metabolite Ndesmethyl enzalutamide in patients with metastatic castrationresistant prostate cancer. J Chromatogr B Analyt Technol Biomed Life Sci 2017; 1058: 102-7. http://dx.doi.org/10.1016/j.jchromb.2017.04.014 PMID: 28545929
- [29] Ortiz-Bolsico C, Torres-Lapasió JR, García-Álvarez-Coque MC. Simultaneous optimization of mobile phase composition, column nature and length to analyse complex samples using serially coupled columns. J Chromatogr A 2013; 1317: 39-48. http://dx.doi.org/10.1016/j.chroma.2013.06.035 PMID: 23845758
- [30] Joseph JA, Akkermans S, Van Impe JFM. Processing method for the quantification of methanol and ethanol from bioreactor samples using gas chromatography-flame ionization detection. ACS Omega 2022; 7(28): 24121-33. http://dx.doi.org/10.1021/acsomega.2c00055 PMID: 35874265
- [31] Acevedo-García V, Padilla-Rascón C, Díaz MJ, Moya M, Castro E. Fermentable sugars production from acid-catalysed steam exploded barley straw. Chem Eng Trans 2018; 70: 1939-44. http://dx.doi.org/10.3303/CET1870324

- [32] Sreejith M, Prashant S, Benny S, Aneesh TP. Preparation of Biological Samples for SEM: Techniques and Procedures. Microscopic Techniques for the Non-Expert. Cham: Springer International Publishing 2022; pp. 227-41. http://dx.doi.org/10.1007/978-3-030-99542-3_10
- [33] Fülöp L, Ecker J. An overview of biomass conversion: Exploring new opportunities. PeerJ 2020; 8: 9586. http://dx.doi.org/10.7717/peerj.9586 PMID: 32765969
- [34] Li W, Zhang X, Chen R, et al. HPLC fingerprint analysis of Phyllanthus emblica ethanol extract and their antioxidant and anti-inflammatory properties. J Ethnopharmacol 2020; 254: 112740. http://dx.doi.org/10.1016/j.jep.2020.112740 PMID: 32151757
- [35] Osorio-González CS, Gómez-Falcon N, Sandoval-Salas F, Saini R, Brar SK, Ramírez AA. Production of biodiesel from castor oil: A review. Energies 2020; 13(10): 2467. http://dx.doi.org/10.3390/en13102467
- [36] Vargas-Ramirez JM, Haagenson DM, Pryor SW, Wiesenborn DP. Determination of suitable storage conditions to preserve fermentable sugars in raw thick beet juice for ethanol production. Biomass Bioenergy 2013; 59: 362-9. http://dx.doi.org/10.1016/j.biombioe.2013.07.014
- [37] Adnan NAA, Suhaimi SN, Abd-Aziz S, Hassan MA, Phang LY.

- Optimization of bioethanol production from glycerol by Escherichia coli SS1. Renew Energy 2014; 66: 625-33. http://dx.doi.org/10.1016/j.renene.2013.12.032
- [38] Tuttle AR, Trahan ND, Son MS. Growth and maintenance of Escherichia coli laboratory strains. Curr Protoc 2021; 1(1): 20. http://dx.doi.org/10.1002/cpz1.20 PMID: 33484484
- [39] Schlusselhuber M, Girard L, Cousin FJ, et al. Pseudomonas crudilactis sp. nov., isolated from raw milk in France. Antonie van Leeuwenhoek 2021; 114(6): 719-30. http://dx.doi.org/10.1007/s10482-021-01552-4 PMID: 33715105
- [40] Simonin H, Beney L, Gervais P. Sequence of occurring damages in yeast plasma membrane during dehydration and rehydration: Mechanisms of cell death. Biochim Biophys Acta Biomembr 2007; 1768(6): 1600-10. http://dx.doi.org/10.1016/j.bbamem.2007.03.017 PMID: 17466936
- [41] Jeong GJ, Khan F, Tabassum N, Cho KJ, Kim YM. Bacterial extracellular vesicles: Modulation of biofilm and virulence properties. Acta Biomater 2024; 178: 13-23. http://dx.doi.org/10.1016/j.actbio.2024.02.029 PMID: 38417645
- [42] Landari H, Roudjane M, Messaddeq Y, Miled A. Pseudo-continuous flow FTIR system for glucose, fructose and sucrose identification in Mid-IR range. Micromachines 2018; 9(10): 517. http://dx.doi.org/10.3390/mi9100517 PMID: 30424450